IEEE Access
Multidisciplinary | Rapid Review | Open Access Journal

Received 4 August 2022, accepted 18 August 2022, date of publication 1 September 2022, date of current version 23 September 2022.

Digital Object Identifier 10.1109/ACCESS.2022.3203586

RESEARCH ARTICLE

An Evolutionary-Neural Mechanism for Arrhythmia Classification With Optimum Features Using Single-Lead Electrocardiogram

AMNAH NASIM[1], (Member, IEEE), DAVID C. NCHEKWUBE[2], (Graduate Student Member, IEEE), FARZEEN MUNIR[3], (Graduate Student Member, IEEE), AND YOON SANG KIM[1], (Member, IEEE)

[1]Department of Computer Science and Engineering, Institute for Bio-Engineering Application Technology, KOREATECH, Cheonan-si 31253, Republic of Korea
[2]Department of Information Engineering, Marche Polytechnic University, 60131 Ancona, Italy
[3]School of Electrical Engineering and Computer Science, Gwangju Institute of Science and Technology, Gwangju 61005, Republic of Korea

Corresponding author: Yoon Sang Kim (yoonsang@koreatech.ac.kr)

This work was supported in part by the Postdoctoral Scholarship Program of KOREATECH.

ABSTRACT Potentially lethal heart abnormalities can be detected/spotted with recent evolution in continuous, long-term cardiac health monitoring using wearable sensors. However, the huge data accumulated presents a challenge in terms of storage, knowledge extraction and computing time. Moreover, manual examination of long-term ECG recordings presents various problems like huge time and work demand, inter-observer variations and difficulty classifying complex non-linear single-lead ECG signal. To address these problems, we propose an automatic heartbeat classification system that uses the optimized minimum number of features using ECG time-series amplitude directly as input, without feature extraction and provides a primary classification and diagnosis for 1 normal and 14 types of arrhythmic heartbeats. Multi-objective particle swarm optimization (MOPSO) is used to achieve the best feature fitness. A novel fitness function is designed to be the sum of macro F1 loss and normalized dimension, with the optimization objective calculated as the minimum of the fitness function. Multi-layer perceptron (MLP), k-nearest neighbor, support vector machine, random forest and extra decision tree classifiers are trained using the selected features. For the targeted 15-class classification problem, MOPSO-optimized features with MLP consistently performed best with significantly reduced number of features. The proposed method proves to be an efficient and effective arrhythmia identification system for continuous, long-term cardiac health monitoring using single-lead ECG signal.

INDEX TERMS Arrhythmia, decision support system, electrocardiogram, feature optimization, multi-objective, particle swarm.

I. INTRODUCTION

Cardiovascular diseases (CVDs) consistently remain the leading cause of death worldwide despite the latest computer-aided diagnosis methods and an evolutionary shift in the increased use of wearable medical devices. World Health Organization (WHO) estimates that 17.9 million people died from CVDs in 2019 worldwide, constituting 32% of the global death count. Of these, an estimated 7.3 million death were due to Coronary Heart Disease (CHD) and 6.2 million were due to stroke. WHO projects that by 2030, almost 23.6 million people will die from CVDs, mainly from heart disease and stroke [1]. A 2021 statistics report by American Heart Association states CHD as the leading cause (42.1%) of deaths attributable to CVDs in the US, followed by stroke (17.0%), high blood pressure (11.0%), heart failure (9.6%), diseases of the arteries (2.9%), and other CVDs (17.4%) [2]. Due to the sudden and highly unpredictable nature of an arrhythmia event, critical i.e., leading to death called sudden cardiac death or non-critical i.e., leading to survival called sudden cardiac arrest, the only prevention and treatment option is to detect and diagnose the particular

The associate editor coordinating the review of this manuscript and approving it for publication was Sotirios Goudos.

CVD condition as early as possible so that management with medicines and behavioural change counselling (smoking, nutrition, exercise, sedentary lifestyle) can begin can begin.

Traditional in-clinic ECG machines is a instantaneous cardiac condition from the standard clinical 10-second test. However, with novel wearable ECG devices, long-term and continuous monitoring is possible. This is an advantage as 10-second tests may fail to identify critical or non-critical events that occur outside the recording window unlike wearable sensors with higher recording frequency [3], [4], [5]. ECG signals acquired with wearable sensors are often lased with distortions which eventually imply a significant computing overhead that necessitate the use of high-end hardware.

Huge amount of data make using automated analysis a challenge; noise from skin contact, muscle activity; individual human factors play a critical role with different subjects having different medical histories and underlying physiological and behavioral conditions. Even for one testing human, ECG signal morphology is not stationary as is also evident by the biometric identification applications of ECG [6], [7], [8]. Then physical activities also contribute to the challenge with processing the signals. Nonlinearity of ECG signals with noise and artefact effect can lead to overlooked or hidden of measured symptoms of diseases and all these in the end culminate in an inaccurate diagnosis. These factors make the risk of getting an incorrect diagnosis of arrhythmia greater.

To meet a medical standard and clinically accepted monitoring system, early detection of abnormal conditions, accurate decision support and high quality and real-time patient data acquisition need to be considered. Computer-aided techniques in this domain work as a decision support tool that provide an accurate and timely diagnosis of heart abnormalities and play a pivotal role in referring the patient to conduct a specialized and detailed assessment of the underlying cause and hence follow a proper prescribed treatment and preventive care. Optimized feature selection could *aid* devices that are able to make long-term and continuous monitoring [9], [10], [11]. Optimum feature selection - removal of noisy and redundant data plus the use of only relevant and least possible amount of data for processing - are realized through the use of advanced processing.

Currently proposed arrhythmia classification systems [12], [13], [14] usually follow pre-processing, QRS detection, cardiac cycle identification, feature definition and extraction and heartbeat classification into normal and multiple types of arrhythmia classes [15], [16], [17], [18], [19]. Recently, researchers have presented different feature reduction methods to reduce input dimensions of ECG signals for neural classifiers. To name a few, Zhang *et al.* [20] extracted statistical features applying the combined method of frequency analysis and Shannon entropy and used information gain criterion to select 10 highly effective features to obtain a good classification on five types of heartbeats. Yildrim *et al.* [21] implemented a convolutional auto-encoder based nonlinear compression structure to reduce the feature size of arrhythmic beats. Tuncer *et al.* [22] applied the neighborhood component analysis feature reduction technique to obtain 64, 128 and 256 features from a 3072 feature vector size. Wang *et al.* [23] proposed effective ECG arrhythmia classification scheme consisting of a feature reduction method combining principal component analysis with linear discriminant analysis. Alonso-Atienza *et al.* [24] used a filter-type feature selection procedure was proposed to analyze the relevance of the computed parameters. Chen and Yu [25] applied nonlinear correlation-based filters, calculated feature–feature correlation to remove redundant features prior to the feature selection process based on feature–class correlation. Asl *et al.* [26] proposed feature reduction scheme based on generalized discriminant analysis. Haseena *et al.* [5], [27] used a fuzzy C-mean (FCM) clustered probabilistic neural network (PNN) for the discrimination of eight types of ECG beats. The performance has been compared with FCM clustered multi layered feed forward network trained with back propagation algorithm. Important parameters parameters are extracted from each ECG beat and feature reduction has been carried out using FCM clustering. Polato *et al.* [28] used principal component analysis. Genetic algorithms have also been applied recently for the optimization of ECG heartbeat features [29], [30], [31], [32] and proved to be advantageous in improving the time-cost value in heartbeat classification methods. Yildirim *et al.* [33] used a DNN model to classify 7 rhythm categories reduced due insufficient recording for 4 cases, from an original 11 classes. The architecture comprised two parts of representation learning with 1D convolutional and sub-sampling layers, and a sequence learning part using long short-term memory (LSTM). In [34] a combination of a radial basis function process neural network (RBF-PNN) and learning vector quantization network (LVQN) was proposed. The first is used to embed prior feature knowledge whereas the later is a competitive learning and structural self-organizing mechanism that expanded the model depth. LVQN measures feature similarities between input signals and pattern category is determined by a set of wining neurons connected to the output. RBFPNN performs spatial-temporal feature aggregation and learning was done by dynamic time warping and C-means clustering. Wang *et al.* [35] proposed an end-to-end deep multi-scale fusion convolutional neural network (DMSFNEt) classification architecture using multiple convolution kernels for feature extraction. The architecture starts with a multi-scale (low to higher scale) feature learning and fusion, then the model is trained by jointly optimizing the losses of multiple branches for effective learning and discriminative classification features. To restore balance to imbalanced dataset [36] used a generative adversarial network (GAN), and a 2-stage deep-CNN performed feature extraction and reduction as well as classification. However, the GAN has a problem of focusing on dominant classes and generation of problematic samples which require extra processing. In [37] the proposed architecture combined parametric features of ECG (amplitude, interval and duration) with visual morphology features. The feature vectors were used to train a NN, SVM and KNN for classification. In [38] a

Gaussian assisted signal smoothing was proposed to increase the peak signal-to-noise ratio followed by a two-stage multi-class CNN. A quadratic SVM was further used to classify signals to respective sub-classes. The classification had 7 sub-classes and 4 main classes. A deep learning framework CNN with point-wise convolution and depth-wise separable convolution was proposed in [39]. Segmented beats were stored as 2D images after annotations. Discrete wavelet transform was used for noise removal. To handle data imbalance [40] proposed a depth-wise separable CNN with focal loss. The focal loss improved especially the small sample cases – the minority classes, and the convolution layers reduce number of parameter selection. Focal loss added weights to the majority and minority samples with a modulating factor. Li *et al.* [41] proposed an image-based setup using deep convolutional neural networks and transfer learning. It used the Inception-V3 model architecture after comparison with resnet, densenet, xception, inception and NASnet models. Jha *et al.* [42] proposed a data compression method based on tunable-Q wavelet transform with Q-factor chosen according to the oscillatory behaviour of the signal. Maximum energy of the signal was compacted to fewer transform coefficients, then followed a dead-zone quantization, integer conversion of coefficients and run length encoding. Features were extracted from the compressed ECG signal. An image analysis was proposed in [43], combining a vector quantized variational autoencoder (VQ-VAE) and a 2D-CNN. VQ-VAE a flexible generating tool for data imbalance. ECG image slices were used to train the PixelCNN classifier. It lacks in interpretability of the rare cases. Luo *et al.* [44] proposed a hybrid convolutional recurrent neural net that processes time-series ECG signal and aimed to solve large imbalance in samples by a synthetic minority oversampling technique. It calculates nearest neighbors by Euclidean distance between data. The RNN comprised layers of a CNN, LSTM and gated recurrent unit (GRU). Du *et al.* [45] proposed a variational autoencoder (VAE) and auxiliary classifier generative adversarial network (ACGAN) to learn data distribution and synthesize images from minority class. CNN classifiers were employed to recognize arrhythmias using 2D ECG images.VAE and ACGAN required to be trained separately highlighting higher computational cost. In [46] an improvement on NN-based classifiers was proposed with a CNN incorporating fine-tuning of attention maps to resemble the ground-truth labels using an L2-distance objective function. Park *et al.* [47] used a squeeze-and-excitation (SE) residual network with 152 layers to categorize 14 classes. The SE block explained model interaction between local parts on entire ECG. An adaptive method was proposed by Bognar and Fridli [48] based on modeling ECG signals with variable rational orthogonal projections employing Malmquist-Takenaka systems of rational functions. The system is a task-specific optimization that builds a feature vector based on dynamic and morphological descriptors (patient-depending and individual-heartbeat-depending features). SVM was used for classification into 5 and 16 classes, and the pole optimization process was time-consuming. An artificial intelligence based diagnosis system was proposed in [49] using texture feature of 2D images of ECG. The images were constructed by projecting the signal vector as a row of the image. A 12-bit signal is transformed into a 8-bit resolution grayscale sub-image on the claim that texture features in images contain determinative indicators of various diseases. Ge *et al.* [50] proposed a feature fusion method guided by multi-label correlation and classification with CNN. The labels were calculated based on frequency and Bayesian conditional probability and a multi-label feature vector generated. Shi *et al.* [51] proposed a classification system based on deep CNN and LSTM network with multiple input layers. Automatic and hand-craft features were both extracted. To manage better the retraining of models, [52] proposed a deep learning-without-forgetting CNN architecture comprising feature extraction module, classification layers, memory module to store prototypes, and a distance matching network task selector module. Taking a ECG converted to image, a pretrained denseNet169 extracted discriminative features.

Most of the cardiac beat classification algorithms proposed in literature (see Section-IV) use computationally intense feature extraction step after the beat segmentation (the beat segmentation criteria may be different than the one used by us i.e., some authors use 5, 6 or 10-second signal classifying rhythm rather than exact beat labels as provided by MIT-BIH data) such as frequency transforms [22], [29], [50], [70], [74], [77], [78], [79], higher-order statistics [70], [78], [79], [80], CNN [36], [38], [39], [40], [43], [44], [51], and others. Feature extraction has to be implemented on every section of the incoming time-series ECG signal being continuously acquired by wearable device (Holter in this case). Hence in the case of ECG signal being acquired in the long-term and continuous monitoring 24-hour acquisition scenarios, the least computationally intensive procedure providing a quick scanning method is to directly identify incoming beats for normal and pathological conditions. None of the abovementioned works use direct beat samples, remove the redundant and noisy features to maximize the performance of discrimination of 15 heartbeat classes additionally considering the imbalanced nature of normal to pathological heart condition occurrence. So according to our best understanding the proposed algorithm takes the route of least computation performing best heartbeat pathology detection for a quick and early reference in case of long-term and continuously acquired ECG for cardiac health monitoring of patients. In the foregoing propositions, a common denominator is the challenge of complexity, scale, computational demand, time cost, interpretability, etc. while maintaining a high overall accuracy of the classification system. Hence, motivated by designing an automated arrhythmia recognition system competitive with the parallel research, in this work, an efficient decision support system was developed to perform a quick scan on the single-lead minimally pre-processed ECG time-series signal acquired by Holter device to detect and recognize a broad range (i.e. 15 classes) of heart abnormality

conditions. The key objective was to improve the accuracy of cardiac arrhythmia classification and analyze the performance of the time-series and their equivalent reduced-sized optimum features of ECG heartbeats. The proposed MOPSO (Multi-objective particle swarm optimization) algorithm is tuned to find an optimum reduced combination of features that performs better as compared to all features. We mainly used PSO because this algorithm has a strong capability to explore a large search space to find global optima rarely falling into local optima thus a good choice for feature selection in the current problem this work distinguishes a wide range of arrhythmia classes. Also, MOPSO uses less computational resource because of fast convergence ability with fewer control parameters. Less computationally efficient algorithms are used at the classification end to test the goodness of reported optimized features. Classification using multi-layer perceptron (MLP) [53], K-nearest neighbor (KNN) [54], support vector machine (SVM) [55], [56], random forest (RF) [57], and decision extra tree (DET) [58] is performed with optimum and all features to show the difference. Using the proposed method for classifying abnormal heartbeats using reduced direct signal amplitude features skips the computation of secondary features, produces higher classification performance due to removal of unnecessary features and is faster in unseen test data due to optimized minimum features.

Summarily, the aim of this research is the realization of the following:

- A novel and effective decision support system for automatic recognition of a broad range of arrhythmia pathologies based on single-lead ECG signals.
- An algorithm using minimum computational complexity in both pre-processing and recognition stages to be applicable for long-term and continuously acquired ECG signals.
- A detailed analysis of the trade-offs of using a minimum number of feature points and classification performance.

II. MATERIALS AND METHODS

The proposed methodology as graphically shown in Fig. 1 follows four steps; 1) preprocessing, 2) beat identification and normalization, 3) MOPSO feature optimization, and 4) disease-based classification. Fig. 2 shows the sample beats for fifteen ECG beat classes. The ECG database and each step of the proposed methodology is discussed in the following.

A. ECG DATABASES

Two datasets MIT−BIH arrhythmia database (MITDB) [63], [64] and MIT−BIH Supraventricular arrhythmia database (MITSVDB) [64], [65] publicly available on PhysioNet.org were used in concatenation for the purposes of testing the effectiveness of the proposed method. The first dataset MITDB consists of 48 two-channel ambulatory ECG records, each of approximately 30 minutes duration digitized at a sampling rate of 360 Hz and gain of 200 analog-to-digital converter units per millivolt (adu/mV), acquired from 47 subjects out of which 25 subjects were men aged 32 to 89 years, and 22 were women aged 23 to 89 years (record number 47 and 48 came from the same subject). Each record has simultaneous recordings from 2 leads, MLII and V5. Hence for this research, 12060 heartbeats are used having corresponding labels for 14 classes i.e. normal (N), left bundle branch block (L), right bundle branch block (R), premature ventricular contraction (V), atrial premature contraction (A), paced (P), ventricular escape (E), fusion of ventricular and normal (F), junctional premature (J), junctional escape (j), aberrated atrial premature (a), non-conducted P-wave (x), ventricular flutter wave (Vf), and fusion of paced and normal (f). The second dataset MITSVDB includes 78 half-hour ECG recordings chosen to increase the examples of supraventricular arrhythmic instances in the MITDB. Each record in MITSVDB is approximately 30 minutes long and contains 2 leads, each sampled at 128 Hz, with a fixed gain of 200 adu/mV. For this research, 9900 heartbeats are used having corresponding labels for 5 classes i.e. normal (N), supraventricular premature (S) and premature ventricular contraction (V). The 78 records made publicly available for standardized testing include pathological conditions such as supraventricular and ventricular arrhythmia. Each record in MITSVDB is resampled to 360 Hz to match the sampling frequency of recorded signals in MITDB. The selected 16 classes include less frequent but clinically significant arrhythmic beats too to prove the validity of the proposed algorithm. Each record in MITDB and SVDB is supported by an annotation file providing the R-peak positions and corresponding beat labels (*Lb*). These class annotations for heartbeats were exploited as reference annotations for evaluation purpose of the proposed model. For the purpose of testing a wearable ECG sensing scenario which mostly uses single-lead for acquisition [66], [67], this work uses ECG signal from only the MLII lead for MITDB and 'ECG1' signal from SVDB. The general characteristics of MITDB and SVDB are summarized in Table.2. The standard Physionet annotations according to ANSI/AAMI EC57:1998 standard [59] and the number of beats randomly picked from corresponding records are detailed in Table.3.

B. PREPROCESSING

The raw ECG signal is acquired through Holter device and the effective ECG frequency lies between 0.5 and 40 Hz frequency band [62]. There is a baseline drift from patient breathing. Hence, in the preprocessing stage, power and low-frequency components are removed from the raw ECG signal by using a 6^{th}-order bidirectional Butterworth band-pass filter with lower and upper cut-off frequencies of 0.5 and 40 Hz, respectively. Next, the baseline is computed as a cubic spline interpolation of fiducial points placed 90 milliseconds before R-peak positions as an approximation for baseline PR-segment and subtracted from the bandpass-filtered signal as shown in Fig. 3.

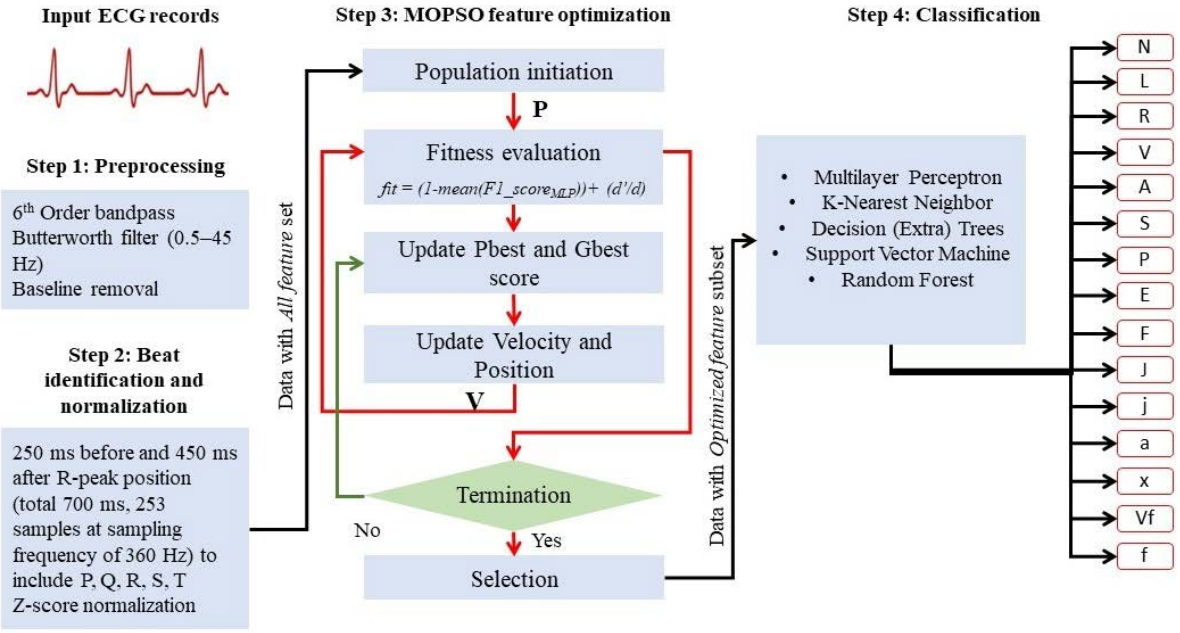

FIGURE 1. Architecture of proposed methodology.

C. BEAT IDENTIFICATION AND NORMALIZATION

Using the R-peak positions provided with each record, a heartbeat sample is identified as having onset 250 ms before each R-peak position to 450 milliseconds after each R-peak position. This definition allows that the important characteristic points of ECG like P, Q, R, S and T waves are included [60]. We utilize the Z-score normalization method to compensate for intersubject differences by first subtracting mean value from each ECG sample, and then dividing by its standard deviation [23]. This procedure results in a normalized ECG sample with zero mean and unity standard deviation. Fig. 3 shows the beat identification from raw ECG signal and preprocessed ECG signal to cardiac cycle identification.

D. MOPSO FEATURE OPTIMIZATION

Features optimization is an integral step in the pipeline shown in Fig. 1. The distribution of normal and abnormal heartbeats is highly unbalanced in the data. The identification of key features for precise detection and categorization of abnormal heartbeats is aided by feature minimization and optimization. Consequently, MOPSO is implemented for optimal feature selection to classify abnormal heartbeats. The MOPSO architecture for feature optimization is depicted in Fig. 4. The computation steps are explained as follows:

1) POPULATION INITIATION

An initial particles matrix **P** is generated as in (1) and (2) to represent the possible solution/optimization space consisting of n_p number of binary row vectors **p** called swarm particles each of length d (number of features in heartbeat samples in this case 253 as mentioned in Section-II-C).

$$P_{n,d} = \begin{bmatrix} p_1 \\ p_2 \\ . \\ . \\ p_i \\ . \\ . \\ p_{n-1} \\ p_n \end{bmatrix} \tag{1}$$

$$P_{i,j} = \begin{bmatrix} p_{1,1} & p_{1,2} & . & . & p_{1,d} \\ p_{2,1} & p_{2,2} & . & . & p_{2,d} \\ . & . & . & & . \\ . & . & . & & . \\ p_{i,1} & p_{i,2} & . & p_{i,j} & p_{i,d} \\ . & . & . & & . \\ . & . & . & & . \\ p_{n-1,1} & p_{n-1,2} & . & . & p_{n-1,d} \\ p_{n,1} & p_{n,2} & . & . & p_{n,d} \end{bmatrix} \tag{2}$$

where, $p_{i,j}$ represents bit value at j^{th} feature position in i^{th} swarm particle. Here $j = 1$ to d and $i = 1$ to n. (2) is a version of (1) for the case where $j = 1$ to d number of features and $i = 1$ to n. 1's and 0's in each swarm particle represent the selected and non-selected features respectively. The number of individuals n is chosen as 50 so that it is large enough to avoid stagnancy and small enough to avoid excessive computing time [61].

2) FITNESS EVALUATION FUNCTION

The particles in the swarm are evaluated using the fitness function. We have used a novel approach and employed the MLP classifier as the fitness function. MLP is a feedforward

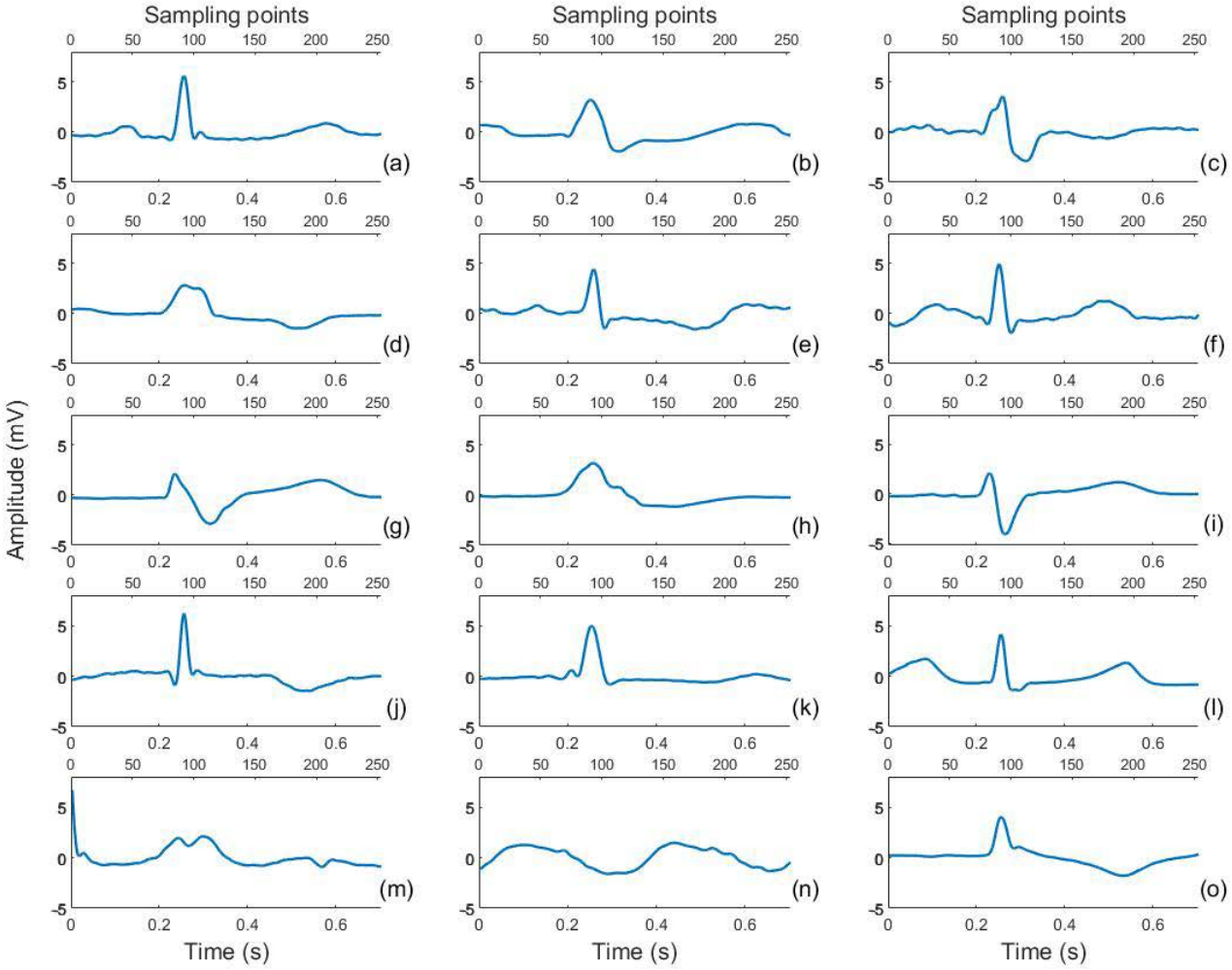

FIGURE 2. Sample beats for fifteen ECG beat classes: (a) normal, (b) left bundle branch block, (c) right bundle branch block, (d) premature ventricular contraction, (e) atrial premature contraction, (f) supraventricular premature, (g) paced, (h) ventricular escape, (i) fusion of ventricular and normal, (j) nodal (junctional) premature, (k) nodal (junctional) escape, (l) aberrated atrial premature, (m) non-conducted P-wave (blocked APB), (n) ventricular flutter, (o) fusion of paced and normal.

neural network consisting of seven layers, i.e., input layer, four hidden layers, and output layer. The input layer has the same size as of feature vector i.e., 253; the hidden layers are of sizes of [220, 180, 120, 60] and the output layer is a size of 15 neurons as depicted in Fig. 5. ReLU activation function is used, and Adam solver is used as an optimizer. The set of selected features from MOPSO iteration is split in training and validation subsets and as in Fig. 6. The MLP classifier is trained and validated on these subsets respectively.

The classification prediction obtained from the validation set is used to calculate *fit* given by (3). *fit* considers one versus rest strategy taking all 1 class as positive and the rest of 14 classes as negative for each individual class. All feature subsets represented by $\mathbf{p}$ in $\mathbf{P}$ are selected from the dataset and individually trained using MLP, and *fit* is calculated on the validation set.

$$fit = min\left((1 - \frac{1}{N}\sum_{c=1}^{N} F1_c) + \frac{d'}{d}\right) \tag{3}$$

$$Macro - F1 = \frac{1}{N}\sum_{c=1}^{N} F1_c,$$
$$F1 = \frac{2 \cdot TP}{2 \cdot TP + FP + FN} \tag{4}$$

where, d' is the reduced number of features selected or number of 1's in the population individual being tested. d is the maximum number of features or the exact length of population individual i.e., 253 in this case. The 1^{st} objective $1 - \frac{1}{N}\sum_{c=1}^{N} F1_c$ is the macro-averaged F1-loss where all classes treated equally. Macro F1-score gives the same importance to each class, hence appropriate for the current multi-class imbalanced classification task. $\frac{d'}{d}$ is the normalized dimension, a minimum of which is desired as a 2^{nd} objective to find the least optimum number of features. A minimum of the sum of these two objectives is desired as *fit*. TP = number of samples for which positive class was correctly identified, TN = number of samples for which negative class was correctly identified, FP = number of samples

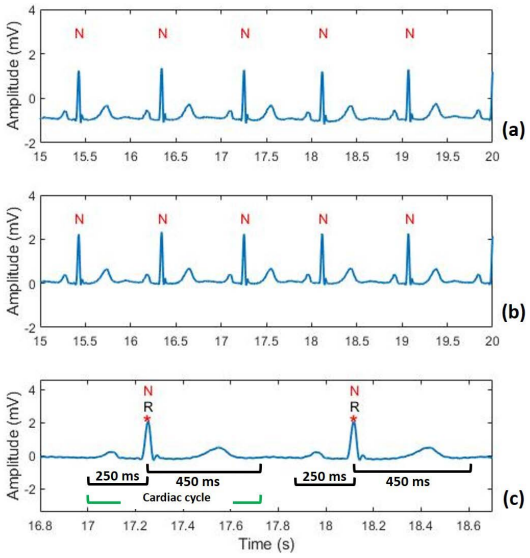

FIGURE 3. Beat identification: (a) Raw ECG signal acquired from Holter with provided beat annotations/labels, (b) Preprocessed ECG signal, and (c) Cardiac cycle identified and consecutively extracted using R-peak positions with corresponding label.

for which positive class was wrongly identified, and FN = number of samples for which negative class was wrongly identified. Hence, FP and FN represent misclassifications or errors made by the classification algorithm. N denotes the total number of classes and $N = 15$ for the current problem.

3) POSITION AND VELOCITY UPDATE

The swarm particles are randomly initialized and then cruised in the search space to search for the optimal features by updating their position and velocity. The particle's position and velocity in search space are denoted as $X_{i,j} = x_{i,1}, x_{i,2}, x_{i,3}, \ldots, x_{i,j}$ and $V_{i,j} = v_{i,1}, v_{i,2}, v_{i,3}, \ldots, v_{i,j}$, where j defines the dimension of search space, and i represents the index of the particle. Updates for velocity, position, weight, best performing particle and fitness value are done using (5), (6), (7), (8) and (9) given as follows:

$$\begin{aligned} V_{i,j}(t) &= w * V_{i,j}(t-1) + C_{i,j} + S_{i,j}, \\ C_{i,j} &= c_1 r_{1,j} * (p_{i,j}(t-1) - x_{i,j}(t-1)), \\ S_{i,j} &= c_2 r_{2,j} * (g_{i,j}(t-1) - x_{i,j}(t-1)) \qquad (5) \\ x_{i,j}(t) &= x_{i,j}(t-1) + V_{i,j}(t) \qquad (6) \\ w &= wMax - t^{th} * ((wMax - wMin)/n) \qquad (7) \\ p_i(t) &= \begin{cases} p_i(t-1) & \text{if } f(x_i(t) >= f(p_i(t-1))) \\ x_i(t) & \text{otherwise} \end{cases} \qquad (8) \\ g(t) &= \text{argmin}(f(p_1(t)), f(p_2(t), \ldots, f(p_s(t))) \qquad (9) \end{aligned}$$

where, t is the iteration in progress, $r_{1,j}$ and $r_{2,j}$ are randomly chosen from the range of [0, 1]. c_1 and c_2 are acceleration coefficients that control the exploration vs the exploitation and inertia is denoted by w. MOPSO maintains particles memory for the local $p_{i,j}$ and global $g_{i,j}$ best position. The local best position defines the highest performance achieved in that position, and the global best position is defined for the overall swarm. The inertia is updated after each iteration using (7). *wMax* and *wMin* represent upper and lower boundary limit respectively. The inertia weight influences the impact of prior velocity on finding the optimal features. Hence, exploration is favored for large inertia weights, and exploitation is favored for smaller values. Algorithm 1 represents a MOPSO based feature reduction.

Algorithm 1: MOPSO Pseudo-Code for Feature Selection

input : A randomly initialize population by creating binary mask for feature indexes ∈ [0, 252]
output: Selection of features by applying global mask and choosing features with binary mask of 1.

Initialize the particles randomly with swarm size of $n_c = 50$;
while $t \leq T$ *or gBestScore does not change for 20 iteration* **do**
  for i **to** n_c **do**
    Evaluate the swarm particle using the fitness function to obtain fit as in (3)
    if $pBestScore_i \geq fit(p_i)$ **then**
      $pBestScore_i \leftarrow fit(p_i)$
      $pBest_i \leftarrow p_i$
    else
      $pBestScore_i \leftarrow pBestScore_i$;
    if $gBestScore_i \geq fit(p_i)$ **then**
      $gBestScore_i \leftarrow fit(p_i)$
      $gBest_i \leftarrow pBest_i$
    else
      $gBestScore_i \leftarrow gBestScore_i$;
    update the velocity in each particle using (5) *and update the mask by applying the new velocity to* (6)
    update inertia weight w using (7)
  return *gBestScore*, *gBest*

4) SELECTION

Fitness function *fit* for each particle in the swarm is calculated using (3). Applying the current-to-best strategy, if p_i shows a higher *fit* value than the corresponding p_i, then p_i in the P is replaced with v_i. Otherwise, the p_i retains its position. This comparison and replacement process is repeated for every (p_i, v_i) pair an evolved version of P is obtained at the end of the iterations. This process evolves and accumulates better particles until the maximum number of iteration i.e. 100 is reached. After looping through all iterations every particle in the P is replaced with the best possible candidate i.e having highest *fit* value. *gBest* with best *fit* in the end p is selected as the optimum feature subset with 1's representing the selected features d' out of d, where $d' \leq d$.

5) TERMINATION

The process terminates if the maximum number of given iteration 100 is reached or *fit* becomes stagnant for a consecutive 20 iteration. For every new iteration, the values of *gBestScore* and *pBestScore* are updated.

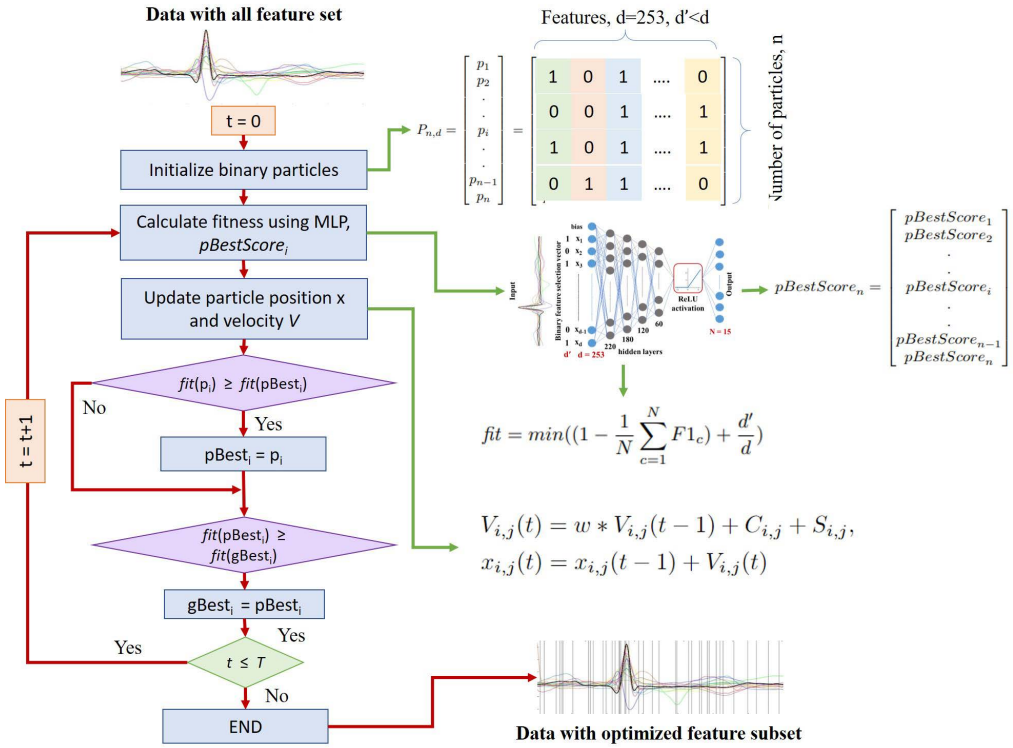

FIGURE 4. MOPSO architecture for feature optimization.

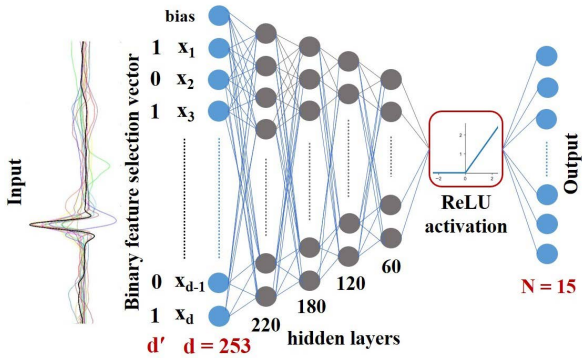

FIGURE 5. MLP architecture to calculate fitness function.

E. CLASSIFICATION

The classification is crucial for the proposed system architecture. It classifies the ECG signal based on the optimized features set obtained from the MOPSO algorithm. We tested five machine learning classifiers for classification with the least hyperparameters and the least possible computational complexity. These classifiers include MLP, KNN, SVM, RF, and DET. MLP architecture is the same as used to calculate *fit* in Section-II-D2.

KNN algorithm is one of the most conventional methods in pattern recognition because of its practical nonparametric nature. The nearest neighbor decision is based on the closest distance a sample has to other K samples. Therefore, euclidean distance is used as a distance measure to classify training samples in the feature space. For experimentation, we have considered a neighborhood size of four sample points.

SVM is a conventional machine learning method in classification. First, the input data are transformed into a high-dimensional feature space. In this space, the data points are linearly separated by a hyper-plane. Because the data points are not linearly separable in most cases, the data points are mapped into a high-dimensional space using an appropriate kernel, and then the optimization step is fulfilled. Various kernel transformations are used to map the data into high-dimensional space, including linear, sigmoid, polynomial, and radial basis functions. We experimented with linear, polynomial, and Radial basis kernels, and the C was set as 100, the Gamma was set as 4, and the polynomial was selected as the kernel-type parameter. This study used parameter optimization to find the optimum SVM parameters.

DET is a predictive model that can characterize both classifiers and regression models. DET refers to a hierarchical model of decisions and their results and is used to classify a sample into a predefined set of classes based on their feature values. DET consists of nodes that form a rooted tree meaning. It is a directed tree with a node called a root with no entering edges. All other nodes have only one entering edge. A node with outgoing edges is referred to as a test node. All other nodes are known as leaves or decision nodes. Each leaf is allocated to one class, demonstrating the most accurate target value. In addition, the leaf holds a probability vector specifying the probability of the target feature with a definite value.

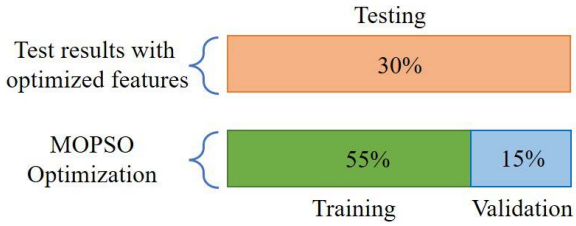

FIGURE 6. Data distribution for training, validation and testing the proposed algorithm for the 15-class disease-specific arrhythmia classification.

Random forests or random decision forests are an ensemble learning method for classification, regression, and other tasks that operate by constructing many decision trees at training time. It uses bagging and feature randomness when building each tree to create an uncorrelated forest of trees whose prediction by committee is more accurate than that of any individual tree. K-Fold grid optimization was used with the number of folds = 5, and the optimum hyperparameters hyperparameters hyperparameters obtained after training for each model are summarized in Table.1.

F. EVALUATION METRICS

Classification metrics; Macro F1-score, accuracy, sensitivity/recall, specificity and precision are reported according to (4), (10), (11), (12), (13) and (14) respectively. All the definitions mentioned below follow a one-versus-rest strategy [68]. Each classification measure is calculated for each of the 15 classes (taking one class as positive and all the rest as negative) and then averaged to represent mean classification measure.

$$Acc = \frac{TP + TN}{TP + TN + FP + FN} \cdot 100 \tag{10}$$

$$Sen = \frac{TP}{TP + FN} \cdot 100 \tag{11}$$

$$Sen_{avg} = \frac{1}{N} \sum_{c=1}^{N} Sen^{(c)} \tag{12}$$

$$Spe = \frac{TN}{TN + FP} \cdot 100 \tag{13}$$

$$Spe_{avg} = \frac{1}{N} \sum_{c=1}^{N} Spe^{(c)} \tag{14}$$

Here, TP, TN, FP and FN follow the same definition as mentioned in Section-II-D2. Fig. 6 shows the data split strategies used for the disease-specific classification case.

III. RESULTS

To test the generalization of finding the optimum features and their applicability we performed a test using all of the 3 above-mentioned datasets. The purpose of this experiment was to test and analyze if the system can optimize and train on the available data and perform well on the unseen incoming ECG signal i.e. test data acquired in a setting different than training. The training data is taken from both MITDB and SVDB. All beats are resampled at 360 Hz and each record in all 2 datasets has been divided by their respective gain to process the signal further in millivolts. The division of records and beats into training and testing sets for an interpatient classification analysis is detailed in Table.3.

TABLE 1. Control parameters.

Parameter	Value
MOPSO	
Swarm size (n)	50
Maximum number of iteration	100
Particle type	Binary bits
Selection scheme	Current-to-best
Particle individual length	253
Acceleration coefficients ($c1$, $c2$)	1.2, 1.2
Inertia weight (ω)	0.24
$c1_{min}, c2_{min}, c1_{max}, c2_{max}$	0.5, 0.5, 2.0, 2.0
$\omega_{min}, \omega_{max}$	0.2, 0.9
MLP	
Optimizer	ADAM
Activation	ReLU
Learning rate	$1e^{-4}$
Input size, output size	253, 15
Hidden layer sizes	220, 180, 120, 60
KNN	
Number of neighbours	4
Weights	distance
DET	
Number of trees	25
Optimum split criterion	entropy
SVM	
kernel	poly
gamma	scale
RF	
Number of trees	25
Optimum split criterion	entropy

Detailed comparisons were performed for both checking the robustness of the reduced features and their efficiency and speed of proposed algorithm to find an optimum solution. The classification was performed for *All features* set (as exact solution) and *Optimized features* subset obtained after MOPSO optimization. Hence, all measures are reported for both *All features* and *Optimized features* cases to present a comparison between classification improvement and feature reduction achieved using the proposed method. To perform a comparison for classification accuracy using optimized features on test data, 5 classifiers are used: MLP, KNN, DET, SVM and RF. An introduction to the working principles of all these classifiers has been presented before in Section-II-E.

A. PARAMETER SETTINGS

The optimum hyperparameter values of implemented classifier architectures for MLP, KNN, RF, SVM and DET implemented on the test data for both all and optimized number of features were selected that performed best for all features (exact solution) and the same model was tested with the test data for reduced and all features. The optimized parameters for all classifiers are mentioned in Table.1. We ran the MOPSO optimization for 10 simulation runs for each experiment in Python on a machine with 6 cores (AMD Ryzen 5

TABLE 2. Summary of test databases.

Database	Number of records	Duration per record (minutes)	Sampling frequency (Hz)	Leads available	Leads used	Number of classes
MIT-BIH Arrhythmia	48	30	360	2	ML-II	14
MIT-BIH Supraventricular Arrhythmia	78	30	128	2	ECG1	5

TABLE 3. Description of beat annotations/labels and detailed beat distribution for train and test data.

No	Symbol	Pathological condition	Record ID, [Number of beats]	Number of records			
				Total	Train	Vald.	Test
1	N	Normal sinus rhythm	MITDB: 100, 101, 103, 105, 106, 108, 112, 113, 114, 115, 116, 117, 119, 121, 122, 123, 200, 201, 202, 203, 205, 208, 209, 210, 212, 213, 215, 219, 220, 221, 222, 223, 228, 230, 233, 234 [100 each], MITSVB: 800, 802, 803, 804, 805, 806, 807, 808, 809, 810, 811, 812, 820, 821, 823, 824, 825, 826, 827, 828, 829, 840, 841, 842, 843, 844, 845, 846, 847, 848, 849, 850, 851, 852, 853, 854, 855, 856, 857, 858, 859, 860, 861, 862, 863, 864, 865, 866, 867, 868, 869, 870, 871, 872, 873, 874, 875, 876, 877, 878, 879, 881, 882, 883 [100 each]	10000	5500	1500	3000
2	L	Left bundle branch block	MITDB: 109, 111, 207, 214 [400 each]	1600	880	240	480
3	R	Right bundle branch block	MITDB: 118, 124, 212, 221, 231 [400 each]	2000	1100	300	600
4	V	Premature ventricular contraction	MITDB: 106, 119, 200, 203, 208, 228, 233, MITSVB: 803, 804, 805, 841, 851, 854, 855, 859, 860, 863, 864, 865, 866, 868, 870 [100 each]	2200	1210	330	660
5	A	Atrial premature contraction beat	MITDB: 207 [100], 209, 222, 232 [200 each]	700	385	105	210
6	S	Supraventricular premature beat	MITSVB: 809, 820, 824, 825, 828, 841, 842, 866, 867, 868, 869, 870, 821, 823, 852, 854, 855, 861, 863, 865 [100 each]	2000	1100	300	600
7	/ (P*)	Paced beat	MITDB: 102, 104, 107, 217 [400 each]	1600	880	240	480
8	E	Ventricular escape beat	MITDB: 207 [100]	100	55	15	30
9	F	Fusion of ventricular and normal beat	MITDB: 208, 213 [200 each]	400	220	60	120
10	J	Nodal (junctional) premature beat	MITDB: 134 [20], 234 [40]	60	33	9	18
11	j	Nodal (junctional) escape beat	MITDB: 222 [200]	200	110	30	60
12	a	Aberrated atrial premature beat	MITDB: 201 [80], 202 [10], 210 [10]	100	55	15	30
13	x	Non-conducted P-wave	MITDB: 201 [20], 219 [130]	150	83	22	45
14	! (Vf*)	Ventricular flutter wave	MITDB: 207 [400]	400	220	60	120
15	f	Fusion of paced and normal beat	MITDB: 102 [50], 104, 217 [200 each]	450	248	67	135
			Total	21960	12079	3293	6588

ANSI/AAMI EC57:1998 standard [59] (https://archive.physionet.org/physiobank/annotations.shtml).
* Standard Physionet annotations for paced and ventricular flutter are / and ! respectively but for ease of understanding we use P and Vf in this paper. Vald. = Validation

3600 CPU @ 3.60 GHz), 32 GB memory and Windows 10. In all experiments, the average performance was reported.

IV. DISCUSSION

The proposed algorithm reduces the number of features from 253 to 40 indicating 84.189% reduction in features with 0.62% reduction in the mean F1-score and 0.85% reduction in accuracy and for the 15-class disease-specific classification. The indices of selected 40 feature subset are given in Table.4. The Table.5 shows a comparison of the *Optimized features* achieved using the proposed algorithm with the *All features* standard used as an exact solution. Table.6 shows a detailed class-wise result achieved with the *Optimized features* in comparison to the *All features* standard. Table.7 and 8 show the confusion matrices of prediction results for both *Optimized features* and *All features* cases. The average number of generations by which the optimization is achieved was 40±4 (10 trials). Beyond this number of generations there was not any further significant improvement of the fitness function.

TABLE 4. Indices of selected 40 feature subset.

4,8,20,24,26,27,37,53,55,58,68,71,77,80,84,85, 86,90,91,94,104,109,118,125,142,143,155,158, 166,168,174,176,183,187,190,201,215,224,236,247

Based on Table.5, we can state that although KNN, DET, SVM and RF provided competitive heartbeat recognition results, MLP provided the best evaluation measures among all the classifiers tested in case of both optimized and all features case with 84.189% reduced feature points. SVM provides highest sensitivity for optimized features only 0.218% better than MLP. Table.6 shows the detailed class-wise result for the best performing MLP classifier. Fig. 7 shows timing analysis done for classification of a single test sample. Mean and standard deviation are reported over 10 trials. MLP shows the highest amount of time required to classify a single test sample but has the lowest error rate keeping in view the natural imbalance of data samples for arrhythmia classification

TABLE 5. Overall classification results.

Classifier	Optimized Features				All Features				% Change	
	%Macro-F1 score	%Accuracy	%Sensitivity/Recall	%Specificity	%Macro-F1	%Accuracy	%Sensitivity/Recall	%Specificity	Features	F1 score
MLP	**88.8**	**95.2**	88.1	**99.6**	**90.5**	**95.6**	**90.6**	**99.6**		-0.41
KNN	86.8	94.5	82.9	99.5	87.1	94.7	84.0	99.5		-0.11
DET	85.6	93.6	80.1	99.4	85.8	94.0	80.7	99.4	-84.2	-0.41
SVM	74.2	85.1	**88.3**	98.9	79.0	89.4	90.4	99.2		-4.25
RF	84.6	93.4	79.8	99.4	83.4	93.1	77.8	99.3		+0.08

TABLE 6. Detailed classification results for the best performing MLP classifier.

Class	Optimized Features				All Features				%Samples (Sample number)
	%F1 score	%Sensitivity/Recall	%Specificity	%Precision	%F1 score	%Sensitivity/Recall	%Specificity	%Precision	
N	97.0	96.8	97.6	97.2	97.0	96.6	97.9	97.4	45.5 (3000)
L	98.3	98.5	99.9	98.1	98.5	98.1	99.9	98.9	7.3 (480)
R	92.7	94.8	99.0	90.8	93.6	94.5	99.3	92.8	9.1 (600)
V	93.2	94.9	99.0	91.7	94.7	95.5	99.3	93.9	10.0 (660)
A	89.1	87.6	99.7	90.6	85.2	89.0	99.3	81.7	3.2 (210)
S	96.7	96.3	99.7	97.1	97.3	97.3	99.7	97.1	9.1 (600)
P	99.3	99.6	99.9	99.0	99.2	99.4	99.9	99.0	7.3 (480)
E	93.1	90.0	100.0	96.4	94.7	90.0	100.0	100.0	0.5 (30)
F	84.6	85.0	99.7	84.3	86.1	85.0	99.8	87.2	1.8 (120)
J	78.9	83.3	99.9	75.0	83.3	83.3	100.0	83.3	0.3 (18)
j	77.6	75.0	99.8	80.4	82.4	81.7	99.8	83.1	0.91 (60)
a	65.5	60.0	99.9	72.0	73.0	76.7	99.8	69.7	0.5 (30)
x	90.3	93.3	99.9	87.5	89.1	91.1	99.9	87.2	0.7 (45)
Vf	85.6	81.7	99.8	89.9	90.1	87.5	99.9	92.9	1.8 (120)
f	89.8	84.4	99.9	95.8	94.0	92.6	99.9	95.4	2.0 (135)

TABLE 7. Confusion matrix - Optimized features.

	N	L	R	V	A	S	P	E	F	J	j	a	x	Vf	f
N	2904	1	30	11	12	10	0 b	1	13	2	8	1	2	2	3
L	0	473	1	5	0	0	0	0	0	0	0	0	0	1	0
R	20	0	569	6	0	2	0	0	0	0	0	1	2	2	0
V	11	3	4	626	0	3	0	0	6	0	0	3	1	3	0
A	19	1	4	1	184	0	0	0	0	1	0	0	0	0	0
S	9	0	4	2	1	578	1	0	0	0	0	2	1	1	1
P	0	0	0	0	0	0	478	0	0	0	0	0	0	1	1
E	0	0	0	3	0	0	0	27	0	0	0	0	0	0	0
F	7	1	0	9	0	0	0	0	102	1	0	0	0	0	0
J	2	0	1	0	0	0	0	0	0	15	0	0	0	0	0
j	9	0	1	1	4	0	0	0	0	0	45	0	0	0	0
a	5	0	0	3	1	2	0	0	0	0	0	18	0	1	0
x	0	0	1	0	1	1	0	0	0	0	0	0	42	4	0
Vf	1	1	12	7	0	1	0	0	0	0	0	0	0	98	0
f	2	2	0	9	0	0	4	0	0	1	3	0	0	0	114

TABLE 8. Confusion matrix - All features.

	N	L	R	V	A	S	P	E	F	J	j	a	x	Vf	f
N	2897	0	30	11	28	6	1	0	9	2	7	4	2	2	1
L	0	471	0	6	0	0	0	0	0	0	0	0	0	2	1
R	23	0	567	3	1	1	0	0	0	0	0	10	3	1	1
V	7	4	1	630	3	5	0	0	6	0	0	1	0	3	0
A	13	0	3	2	187	1	0	0	0	1	2	0	0	0	1
S	7	0	4	1	1	584	1	0	0	0	0	1	1	0	0
P	0	0	0	1	0	0	477	0	0	0	0	1	0	0	1
E	0	0	0	3	0	0	0	27	0	0	0	0	0	0	0
F	10	0	0	8	0	0	0	0	102	0	0	0	0	0	0
J	1	0	1	0	0	0	0	0	0	15	1	0	0	0	0
j	6	0	0	1	4	0	0	0	0	0	49	0	0	0	0
a	5	0	0	0	2	0	0	0	0	0	0	23	0	0	0
x	1	0	1	0	1	0	0	0	0	0	0	1	41	0	0
Vf	2	0	4	3	0	3	0	0	0	0	0	2	0	105	1
f	1	1	0	2	2	1	3	0	0	0	0	0	0	0	125

task. Furthermore, for the optimized feature subset the time is even reduced. Compared to KNN, DET, SVM and RF though MLP takes more time even for optimized feature subset. All classifiers show a significant decrease in computing time when comparing optimized feature and all feature case respectively. Fig. 8 (a and c) shows overall ROC curves

TABLE 9. Summary of the latest related literature.

Reference	Feature type	#Classes	Feature reduction	Classification	Accuracy (%)	F1-score (%)
[73]	Temporal VCG	3	PSO	SVM	92.40	-
[71]	k-medoids VQ	4	none	Parallel regression NN	95.00	
[79]	LBP, HOS, CWT, hand-crafted	4	-	MPA-CNN	99.76	94.44
[77]	2D-CWT scalogram	4	-	3-layer 2-D CNN	98.74	68.76
[21]	Morphology	5	CAE	LSTM	99.00	99.00
[70]	HOS+Wavelet	5	ICA+PCA	SVM+NN	98.91	-
[72]	Morphology	5	none	9-layer Deep CNN	94.03	-
[78]	LBP, HOS, wavelet and magnitude	5	MRFO	SVM	98.26	97.82
[33]	Raw	7	Representation learning	CNN, LSTM	92.24	-
[34]	Spatial-temporal morphology, LVQN	7	DTW, C-means	RBFPNN	85.63	86.26
[41]	Image	7	none	Transfer learning deep CNN	98.46	-
[42]	Compressed signal	8	Energy compacting	Tunable-Q wavelet transform	98.37	-
[44]	Time samples	9	SMOTE	CNN,LSTM,GRU	99.01	99.51
[45]	Attention maps	9	L2-distance	CNN	84.50	81.20
[49]	Image texture	9	none	Randomized NN	99.00	-
[50]	Frequency, Bayesian conditional probability	9	Multi-label correlation	CNN	-	82.70
[35]	Raw	10	Multi-scale fusion	CNN	-	82.80
[38]	Smoothed signal	11	none	2-stage CNN, Quadratic SVM	97.63	92.63
[36]	Raw	15	none	GAN, 2-stage CNN	98.00	-
[51]	Time-series CNN	15	none	LSTM	99.26	-
[74]	DCT + weighted inter-beat	5, 15	none	SVM	98.46	-
[37]	Visual morphology + amplitude, interval, duration	15	none	NN, SVM, KNN	97.70	-
[48]	Orthogonal projections	16	Malmquist-Takenaka systems	SVM	99.5	-
[40]	Raw	17	Focal loss	Depthwise separable CNN	98.55	79.00
[29]	PSD+DFT	17	GA	SVM, kNN, PNN, and RBFNN	98.85	-
[22]	Multilevel wavelet	17	NCA	1-NN	95.00	-

for both optimized and all feature scenarios. AUC for the optimized features is 0.996 with a 0.001 or 0.1% reduction in overall AUC as compared to the all-features scenario. Fig. 8 (b and d) shows individual class recognition AUC for both optimized and all feature cases. Recognition AUC for classes normal, right bundle branch block, premature ventricular, premature atrial, ventricular escape, junctional, aberrated atrial premature, fusion of ventricular and normal and ventricular flutter with optimized features decreased by 0.1%, 0.2%, 0.1%, 0.1%, 0.2%, 1.8%, 0.9%, 0.8% and 0.7% and, for classes supraventricular, fusion of paced and normal, nodal junctional and non-conducted P wave increased by 0.2%, 0.3%, 1.6%, 0.3% as compared to the all-features scenario. AUC for classes left bundle branch block and paced remained 100% and unchanged for both cases. These small [0.1-1.8]% positive and negative trade-offs in individual recognition of different cardiac pathologies come at 84.189% reduction in features. This overall arrhythmia detection and recognition for a primary scan check as depicted in Fig. 9 in continuous and long-term cardiac health monitoring applications using single-lead ECG signal successfully proves to be a quick and early referral system to send the patient to a general physician/cardiac specialist or to emergency in case of stroke.

As summarized in Table.9, most of the previous studies perform classification for 3, 4, and 5 arrhythmia classes mostly belonging to AAMI/ANSI heartbeat types i.e., N, S, V, F, and Q or a subset of these. The works focused on achieving maximum accuracy. The problem in this particular case using the accuracy as prediction metric is that normal class has much greater number of samples than arrhythmic samples. Then different types of arrhythmias ventricular, supraventricular, atrial pathologies and their subtypes have different frequency of occurrence some of them rare than others. Accuracy in this case does not put higher importance to the prediction quality of minority classes, which in our case or in the case of disease analysis in general opposes the design objective. Hence, in this work, we worked to achieve macro F1 score which put equal weight to prediction of majority (i.e. normal) and all minority (i.e. arrhythmia) classes.

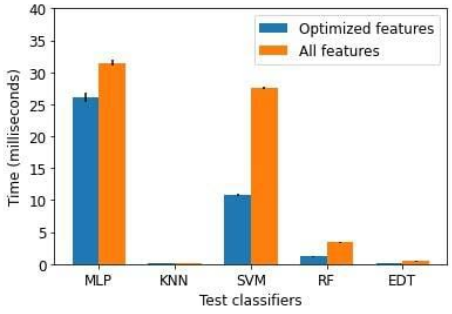

FIGURE 7. Comparison of computing time required to classify 1 test sample using MLP, KNN, SVM, RF and DET.

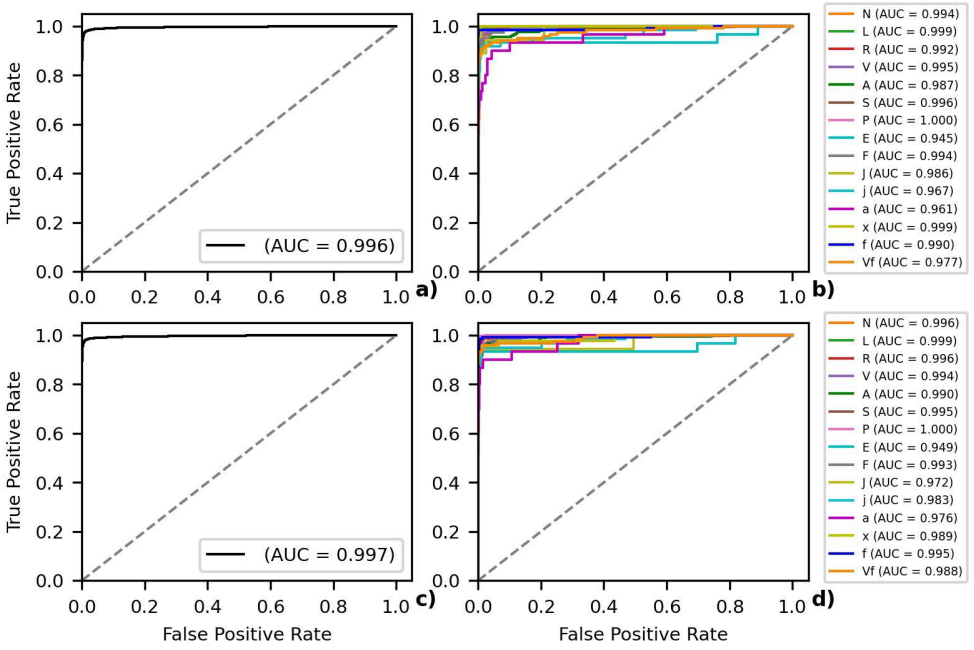

FIGURE 8. ROC curves for: (a) Optimized features - overall, (b) Optimized features - classwise, (c) All features - overall, and (d) All features - classwise.

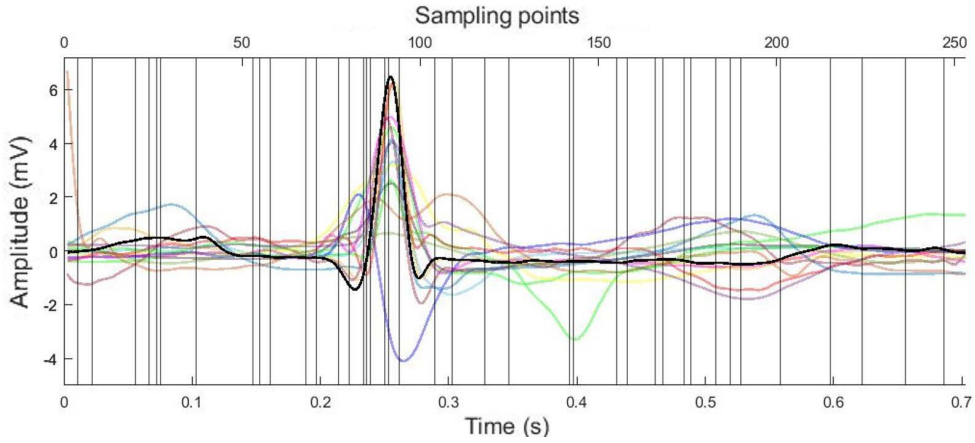

FIGURE 9. Achieved optimized feature scan to discriminate between 15 (1 normal and 14 arrhythmic) types of heartbeats.

Although an exact comparison is not possible as the works that actually performed classification for 15-17 classes worked with 10 second ECG fragments rather than individually segmented beats, also using solely amplitude points as features. For example, Plawiak [29] achieved an accuracy of 98.85% with 90.20% sensitivity classifying 17 classes (1 normal, 15 arrhythmia and 1 unclassifiable beat) using an extensive and complex feature extraction step i.e., power spectral density using Welch's method and discrete Fourier transform. Tuncer *et al.* [22] extracted 3072 (5-levels discrete wavelet transform and 1-dimensional hexadecimal local pattern) dimensional feature set subjected to neighborhood component analysis feature reduction technique to obtain 64, 128 and 256 features. Using KNN classifier with K=1 for classification of 17 arrhythmia classes using MIT-BIH Arrhythmia ECG dataset they obtain an accuracy of 94.6, 94.7, and 95.0% for 64, 128 and 256 features respectively. Yıldırım *et al.* [69] used rescaled raw 10 second signals as features and 16-layer 1D-CNN for classification. They reported accuracy of 95.20, 92.51, and 91.33% for 13, 15 and 17 classes respectively. Hence, to the best of our knowledge, the currently presented results show a competitive best recognition sensitivity for the 15 classes based on MOPSO-MLP scheme to be 88.089%, with 95.21% accuracy meaning 5 errors per 100 classifications.

As summarized in Table.9, most of the works that report an overall F1 score higher than ours [21], [44], [78], [79] performed classification for a limited 2 to 12 heart pathologies, highest F1 being 92.63% achieved by [38] for 11 classes. The current study achieves best F1 score considering 15 class heartbeat recognition. The studies that report high level of accuracy for recognition of 13-17 classes [22], [36], [40],

TABLE 10. Appendix 1: The list of used abbreviations.

Acronym	Meaning
LBP	Local Binary Pattern
HOS	Higher-Order Statistical
PSD	Power Spectral Density
DFT	Discrete Fourier Transform
DCT	Discrete Cosine Transform
MRFO	Manta Ray Foraging Optimization
VCG	Vectorcardiogram
CWT	Continuous Wavelet Transform
PSO	Particle Swarm Optimization
CNN	Convolutinal Neural Network
LSTM	Long Short-Term Memory
AE	Autoencoder
SVM	Support Vector Machine
RF	Random Forest
NN	Neural Network
KNN	K-Nearest Neighbour
DET	Extra Decision Tree
RBFNN	Radial Basis Function Neural Network
LS-SVM	Least Squares SVM
MPA	Marine Predators Algorithm
VQ	Vector Quantization

[51], mostly use 4 to 7-layer deep CNNs for feature extraction which is a highly computationally complex feature extraction method and difficult to perform every time for every single beat especially dealing with 24-hour signal acquisitions. Hence, considering the accuracy, F1, precision of diagnosis, reduction in computational complexity needed for practical applicability of arrhythmia diagnosis systems for arrhythmia, the current work presents a competitive best among the latest studies. The only computationally intensive part is the optimization and in the current procedure it has to happen only once to produce the optimized feature vector. However, there is a limitation that for the currently tested data the sampling frequency of the ECG data acquisition device had a sampling frequency of 360 Hz. For a second database MITSVDB with data acquired from the Holter device but at a sampling frequency of 128 Hz to be concatenated with our test data we had to resample it to 360 Hz. Hence, for devices acquiring ECG data at different sampling frequencies, the signal would need to be resampled for the proposed feature point vector to be usable. The confusion matrices show a high percentage of arrhythmic beats being wrongly classified as normal. This could be due to distortion in the heartbeat amplitudes due to noise or other motion artifacts. In future, we intend to improve the classification performance by first discriminating between normal and abnormal heartbeats and afterwards performing subclass classification for arrhythmia. Also, to make the proposed system to reproduce the ECG signal to be used in a clinic/hospital setting, we intend to work with 10 second segments and multi-label pathological indication provision. Overall the achieved ECG arrhythmia classification result indicates that detection of arrhythmia using 15.81% features of a complete ECG heartbeat can be an effective approach to help general physicians and cardiology specialists to diagnose critical cardiovascular diseases in a continuous and long-term, online or offline monitoring scenarios particularly well-suited for a wearable sensing setting.

V. CONCLUSION

This work focused on reducing the dimension of features to perform a quick scan on heartbeats segmented from single-lead ECG signal for the purpose of abnormal cardiac pathology recognition to be used as an early referral system. The results obtained in all experiments confirmed that the proposed MOPSO-MLP method efficiently delivers competitive recognition performance and precision with 84.189% less time-series amplitude points. Furthermore, the developed method provides early diagnosis for a wide range of heart abnormalities making it an applicable arrhythmia decision support system for wearable ECG devices.

ACKNOWLEDGMENT

The authors would like to thank the guidance and support of Prof. Laura Burattini (Department of Information Engineering, Polytechnic University of Marche, Italy) in conducting this research.

CONFLICT OF INTEREST

The authors declare no conflicting interests in the publishing of this paper.

REFERENCES

[1] World Health Organization (WHO). (2011). *Global Atlas on Cardiovascular Disease Prevention and Control*. Accessed: Dec. 20, 2021. [Online]. Available: https://apps.who.int/iris/bitstream/handle/10665/329516/9789241564373-eng.pdf

[2] S. S. Virani, A. Alonso, H. Aparicio, E. Benjamin, M. Bittencourt, C. Callaway, A. Carson, A. Charmberlain, S. Cheng, and F. Delling, "Heart disease and stroke statistics—2021 update: A report from the American heart association," *Circulation*, vol. 143, no. 8, pp. e254–e743, Feb. 2021.

[3] M. M. Baig, H. Gholamhosseini, and M. J. Connolly, "A comprehensive survey of wearable and wireless ECG monitoring systems for older adults," *Med. Biol. Eng. Comput.*, vol. 51, no. 5, pp. 485–495, Jan. 2013.

[4] C. Davenport, E. Cheng, Y. Kwok, A. Lai, T. Wakabayashi, C. Hyde, and M. Connock, "Assessing the diagnostic test accuracy of natriuretic peptides and ECG in the diagnosis of left ventricular systolic dysfunction: A systematic review and meta-analysis," *Brit. J. Gen. Pract.*, vol. 56, no. 522, pp. 48–56, Jan. 2006.

[5] R. Ceylan and O. Yüksel, "Comparison of FCM, PCA and WT techniques for classification ECG arrhythmias using artificial neural network," *Expert Syst. Appl.*, vol. 33, no. 2, pp. 286–295, Aug. 2007.

[6] A. N. Uwaechia and D. A. Ramli, "A comprehensive survey on ECG signals as new biometric modality for human authentication: Recent advances and future challenges," *IEEE Access*, vol. 9, pp. 97760–97802, 2021.

[7] R. Srivastva, A. Singh, and Y. N. Singh, "PlexNet: A fast and robust ECG biometric system for human recognition," *Infom. Sci.*, vol. 558, pp. 208–228, May 2021.

[8] S. Dalal and V. P. Vishwakarma, "Classification of ECG signals using multi-cumulants based evolutionary hybrid classifier," *Sci. Rep.*, vol. 11, no. 1, pp. 1–25, Jul. 2021.

[9] A. Gacek, "An introduction to ECG signal processing and analysis," in *ECG Signal Processing, Classification and Interpretation: A Comprehensive Framework of Computational Intelligence*, 1st ed. London, U.K.: Springer, Aug. 2011, pp. 21–46, ch. 2, sec. 2.1.

[10] A. Wosiak, "Principal component analysis based on data characteristics for dimensionality reduction of ECG recordings in arrhythmia classification," *Open Phys.*, vol. 17, no. 1, pp. 489–496, Sep. 2019.

[11] B. Remeseiro and V. Bolon-Canedo, "A review of feature selection methods in medical applications," *Comput. Biol. Med.*, vol. 112, Sep. 2019, Art. no. 103375.

[12] V. Sree, J. Mapes, S. Dua, O. S. Lih, J. E. W. Koh, E. J. Ciaccio, and U. R. Acharya, "A novel machine learning framework for automated detection of arrhythmias in ECG segments," *J. Ambient Intell. Hum. Comput.*, vol. 20, pp. 1–18, Jan. 2021.

[13] S. Sahoo, M. Dash, S. Behera, and S. Sabut, "Machine learning approach to detect cardiac arrhythmias in ECG signals: A survey," *Innov. Res. Biomed. Eng.*, vol. 41, pp. 185–194, Aug. 2020.

[14] H. Fujita and D. Cimr, "Decision support system for arrhythmia prediction using convolutional neural network structure without preprocessing," *Appl. Intell.*, vol. 49, no. 9, pp. 3383–3391, Apr. 2019.
[15] S. H. Jambukia, V. K. Dabhi, and H. B. Prajapati, "Classification of ECG signals using machine learning techniques: A survey," in *Proc. IEEE Conf. Adv. Comput. Eng. Appl.*, Jul. 2015, pp. 714–721.
[16] S. K. Berkaya, A. K. Uysal, E. S. Gunal, S. Ergin, S. Gunal, and M. B. Gulmezoglu, "A survey on ECG analysis," *Biomed. Signal Process. Control*, vol. 43, pp. 216–235, May 2018.
[17] E. J. D. S. Luz, W. R. Schwartz, G. Cámara-Chávez, and D. Menotti, "ECG-based heartbeat classification for arrhythmia detection: A survey," *Comput. Methods Programs Biomed.*, vol. 127, pp. 144–164, Apr. 2016.
[18] S. Karpagachelvi, M. Arthanari, and M. Sivakumar, "ECG feature extraction techniques—A survey approach," 2010, *arXiv:1005.0957*.
[19] M. A. Serhani, H. T. El Kassabi, H. Ismail, and A. N. Navaz, "ECG monitoring systems: Review, architecture, processes, and key challenges," *Sensors*, vol. 20, p. 1796, Feb. 2020.
[20] Y. Zhang, Y. Zhang, B. Lo, and W. Xu, "Wearable ECG signal processing for automated cardiac arrhythmia classification using CFASE-based feature selection," *Expert Syst.*, vol. 37, no. 1, p. e12432, Jun. 2019.
[21] O. Yildirim, U. B. Baloglu, R.-S. Tan, E. J. Ciaccio, and U. R. Acharya, "A new approach for arrhythmia classification using deep coded features and LSTM networks," *Comput. Methods Programs Biomed.*, vol. 176, pp. 121–133, Jul. 2019.
[22] T. Tuncer, S. Dogan, P. Pławiak, and U. R. Acharya, "Automated arrhythmia detection using novel hexadecimal local pattern and multilevel wavelet transform with ECG signals," *Knowl.-Based Syst.*, vol. 186, Dec. 2019, Art. no. 104923.
[23] J. S. Wang, W. Chiang, Y. Hsu, and Y. C. Yang, "ECG arrhythmia classification using a probabilistic neural network with a feature reduction method," *Neurocomputing*, vol. 116, pp. 38–45, Sep. 2013.
[24] F. Alonso-Atienza, E. Morgado, L. Fernandez-Martinez, A. García-Alberola, and J. L. Rojo-Alvarez, "Detection of life-threatening arrhythmias using feature selection and support vector machines," *IEEE Trans. Biomed. Eng.*, vol. 61, no. 3, pp. 832–840, Nov. 2013.
[25] Y. Chen and S. Yu, "Selection of effective features for ECG beat recognition based on nonlinear correlations," *Artif. Intell. Med.*, vol. 54, no. 1, pp. 43–52, Jan. 2012.
[26] B. Asl, S. Setarehdan, and M. Mohebbi, "Support Vector machine-based arrhythmia classification using reduced features of heart rate variability signal," *Artif. Intell. Med.*, vol. 44, no. 1, pp. 51–64, Sep. 2008.
[27] H. H. Haseena, A. T. Mathew, and J. K. Paul, "Fuzzy clustered probabilistic and multi layered feed forward neural networks for electrocardiogram arrhythmia classification," *J. Med. Syst.*, vol. 35, no. 2, pp. 179–188, Aug. 2011.
[28] K. Polat and S. Güneş, "Detection of ECG arrhythmia using a differential expert system approach based on principal component analysis and least square support vector machine," *Appl. Math. Comput.*, vol. 186, no. 1, pp. 898–906, Mar. 2007.
[29] P. Pławiak, "Novel genetic ensembles of classifiers applied to myocardium dysfunction recognition based on ECG signals," *Swarm Evol. Comput.*, vol. 39, pp. 192–208, Apr. 2018.
[30] E. H. Houssein, A. A. Ewees, and M. A. ElAziz, "Improving twin support vector machine based on hybrid swarm optimizer for heartbeat classification," *Pattern Recognit. Image Anal.*, vol. 28, no. 2, pp. 243–253, Jun. 2018.
[31] H. Li, D. Yuan, X. Ma, D. Cui, and L. Cao, "Genetic algorithm for the optimization of features and neural networks in ECG signals classification," *Sci. Rep.*, vol. 7, p. 41011, Jan. 2017.
[32] O. Yildirim and U. B. Baloglu, "Heartbeat type classification with optimized feature vectors," *Int. J. Opt. Control, Theories Appl.*, vol. 8, no. 2, pp. 170–175, Apr. 2018.
[33] O. Yildirim, M. Talo, E. J. Ciaccio, R. S. Tan, and U. R. Acharya, "Accurate deep neural network model to detect cardiac arrhythmia on more than 10,000 individual subject ECG records," *Comput. Methods Programs Biomed.*, vol. 197, no. 2, Dec. 2020, Art. no. 105740.
[34] L. Wu, Y. Wang, S. Xu, K. Liu, and X. Li, "An RBF-LVQPNN model and its application to time-varying signal classification," *Appl. Intell.*, vol. 8, no. 51, pp. 4548–4560, Jan. 2021.
[35] R. Wang, J. Fan, and Y. Li, "Deep multi-scale fusion neural network for multi-class arrhythmia detection," *IEEE J. Biomed. Health Informat.*, vol. 24, no. 9, pp. 2461–2472, Sep. 2020.
[36] A. M. Shaker, M. Tantawi, H. A. Shedeed, and M. F. Tolba, "Generalization of convolutional neural networks for ECG classification using generative adversarial networks," *IEEE Access*, vol. 8, pp. 35592–35605, 2020.
[37] H. Yang and Z. Wei, "Arrhythmia recognition and classification using combined parametric and visual pattern features of ECG morphology," *IEEE Access*, vol. 8, pp. 47103–47117, 2020.
[38] A. Chandrasekar, D. D. Shekar, A. C. Hiremath, and K. Chemmangat, "Detection of arrhythmia from electrocardiogram signals using a novel Gaussian assisted signal smoothing and pattern recognition," *Biomed. Signal Proces.*, vol. 73, p. 103469, Mar. 2022.
[39] Y. P. Sai and L. V. R. Kumari, "Cognitive assistant DeepNet model for detection of cardiac arrhythmia," *Biomed. Signal Proces.*, vol. 71, Jan. 2022, Art. no. 103221.
[40] Y. Lu, M. Jiang, L. Wei, J. Zhang, Z. Wang, B. Wei, and L. Xia, "Automated arrhythmia classification using depthwise separable convolutional neural network with focal loss," *Biomed. Signal Proces.*, vol. 69, Aug. 2021, Art. no. 102843.
[41] C. Li, H. Zhao, W. Lu, X. Leng, L. Wang, X. Lin, Y. Pan, W. Jiang, J. Jiang, Y. Sun, J. Wang, and J. Xiang, "DeepECG: Image-based electrocardiogram interpretation with deep convolutional neural networks," *Biomed. Signal Proces.*, vol. 69, Aug. 2021, Art. no. 102824.
[42] C. K. Jha and M. H. Kolekar, "Tunable Q-wavelet based ECG data compression with validation using cardiac arrhythmia patterns," *Biomed. Signal Proces.*, vol. 66, Apr. 2021, Art. no. 102464.
[43] H. Liu, Z. Zhao, X. Chen, R. Yu, and Q. She, "Using the VQ-VAE to improve the recognition of abnormalities in short-duration 12-lead electrocardiogram records," *Comput. Methods Programs Biomed.*, vol. 196, Nov. 2020, Art. no. 105639.
[44] X. Luo, L. Yang, H. Cai, R. Tang, Y. Chen, and W. Li, "Multi-classification of arrhythmias using a HCRNet on imbalanced ECG datasets," *Comput. Methods Programs Biomed.*, vol. 208, Sep. 2021, Art. no. 106258.
[45] C. Du, P. X. Liu, and M. Zheng, "Classification of imbalanced electrocardiosignal data using convolutional neural network," *Comput. Methods Programs Biomed.*, vol. 214, Feb. 2022, Art. no. 106483.
[46] J. Yoo, T. J. Jun, and Y. Kim, "XECGNet: Fine-tuning attention map within convolutional neural network to improve detection and explainability of concurrent cardiac arrhythmias," *Comput. Methods Programs Biomed.*, vol. 208, Sep. 2021, Art. no. 106281.
[47] J. Park, J. An, J. Kim, S. Jung, Y. Gil, Y. Jang, K. Lee, and I. Oh, "Study on the use of standard 12-lead ECG data for rhythm-type ECG classification problems," *Comput. Methods Programs Biomed.*, vol. 214, Feb. 2022, Art. no. 106521.
[48] G. Bognár and S. Fridli, "ECG heartbeat classification by means of variable rational projection," *Biomed. Signal Process.*, vol. 61, Aug. 2020, Art. no. 102034.
[49] O. F. Ertuğrul, E. Acar, E. Aldemir, and A. Öztekin, "Automatic diagnosis of cardiovascular disorders by sub images of the ECG signal using multi-feature extraction methods and randomized neural network," *Biomed. Signal Process.*, vol. 64, Feb. 2021, Art. no. 102260.
[50] Z. Ge, X. Jiang, Z. Tong, P. Feng, B. Zhou, M. Xu, Z. Wang, and Y. Pang, "Multi-label correlation guided feature fusion network for abnormal ECG diagnosis," *Knowl.-Based Syst.*, vol. 233, Dec. 2021, Art. no. 107508.
[51] H. Shi, C. Qin, D. Xiao, L. Zhao, and C. Liu, "Automated heartbeat classification based on deep neural network with multiple input layers," *Knowl.-Based Syst.*, vol. 188, Jan. 2020, Art. no. 105036.
[52] N. Ammour, H. Alhichri, Y. Bazi, and N. Alajlan, "LwF-ECG: Learning-without-forgetting approach for electrocardiogram heartbeat classification based on memory with task selector," *Comput. Biol. Med.*, vol. 137, Oct. 2021, Art. no. 104807.
[53] M. Riedmiller and A. Lernen, "Multi layer perceptron," Mach. Learn. Lab, Univ. Freiburg, Special Lect., 2014, pp. 7–24. Accessed: Dec. 23, 2021. [Online]. Available: https://ml.informatik.uni-freiburg.de/former/_media/documents/teaching/ss12/ml/05_mlps.printer.pdf
[54] G. Guo, W, Hui, B. D. Bell, Y. Bi, and K. Greer, "KNN model-based approach in classification," in *Proc. OTM Confederated Int. Conf.* Berlin, Germany, 2003, pp. 986–996.
[55] V. Cherkassky and Y. Ma, "Practical selection of SVM parameters and noise estimation for SVM regression," *Neural Netw.*, vol. 17, no. 1, pp. 113–126, Jan. 2004.
[56] M., Farzeen, S. Gull, and A. Asif, "MILAMP: Multiple instance prediction of amyloid proteins," *IEEE/ACM Trans. Comput. Biol. Bioinf.*, vol. 18, no. 3, pp. 1142–1150, Aug. 2019.
[57] M. Pal, "Random forest classifier for remote sensing classification," *Int. J. Remote Sens.*, vol. 26, no. 1, pp. 217–222, 2007.

[58] O. Maier, M. Wilms, J. von der Gablentz, U. M. Krämer, and T. F. Münte, "Extra tree forests for sub-acute ischemic stroke lesion segmentation in MR sequences," *J. Neurosci. Methods*, vol. 240, pp. 89–100, Jan. 2015.

[59] *Testing and Reporting Performance Results of Cardiac Rhythm and ST Segment Measurement Algorithms*, Standard ANSI/AAMI EC57, ARPN, 1998.

[60] D. Marinucci, A. Sbrollini, I. Marcantoni, M. Morettini, C. A. Swenne, and L. Burattini, "Artificial neural network for atrial fibrillation identification in portable devices," *Sensors*, vol. 20, no. 12, p. 3570, Jun. 2020.

[61] A. R. Jordehi and J. Jasni, "Parameter selection in particle swarm optimisation: A survey," *J. Experim. Theor. Artif. Intell.*, vol. 25, no. 4, pp. 527–542, Jun. 2013.

[62] M. H. Sedaaghi and M. Khosravi, "Morphological ECG signal preprocessing with more efficient baseline drift removal," in *Proc. 7th. IASTED Int. Conf. (ASC)*, 2003, pp. 205–209.

[63] G. B. Moody and G. M. Roger, "The impact of the MIT-BIH arrhythmia database," *IEEE Eng. Med. Biol. Mag.*, vol. 20, no. 3, pp. 45–50, Jun. 2001.

[64] A. L. Goldberger, L. A. Amaral, L. Glass, J. M. Hausdorff, P. C. Ivanov, R. G. Mark, J. E. Mietus, G. B. Moody, C. K. Peng, and H. E. Stanley, "PhysioBank, PhysioToolkit, and PhysioNet: Components of a new research resource for complex physiologic signals," *Circulation*, vol. 101, no. 23, pp. e215–e220, Jun. 2000.

[65] S. D. Greenwald, R. S. Patil, and R. G. Mark, "Improved detection and classification of arrhythmias in noise-corrupted electrocardiograms using contextual information," in *Proc. Comput. Cardiol.*, Chicago, IL, USA, Sep. 1990, pp. 461–464.

[66] S. M. Mathews, C. Kambhamettu, and K. E. Barner, "A novel application of deep learning for single-lead ECG classification," *Comput. Biol. Med.*, vol. 99, pp. 53–62, Aug. 2018.

[67] F. M. Dias, H. L. M. Monteiro, T. W. Cabral, R. Naji, M. Kuehni, and E. J. Luz, "Arrhythmia classification from single-lead ECG signals using the inter-patient paradigm," *Circulation*, vol. 202, no. 23, Apr. 2021, Art. no. 105948.

[68] J. Xu, "An extended one-versus-rest support vector machine for multi-label classification," *Neurocomputing*, vol. 74, no. 17, pp. 3114–3124, Oct. 2011.

[69] Ö. Yildirim, P. Plawiak, R.-S. Tan, and U. R. Acharya, "Arrhythmia detection using deep convolutional neural network with long duration ECG signals," *Comput. Biol. Med.*, vol. 102, no. 1, pp. 411–420, Nov. 2018.

[70] F. A. Elhaj, N. Salim, A. R. Harris, T. T. Swee, and T. Ahmed, "Arrhythmia recognition and classification using combined linear and nonlinear features of ECG signals," *Comput. Methods Programs Biomed.*, vol. 127, pp. 52–63, Apr. 2016.

[71] T. Liu, Y. Si, D. Wen, M. Zang, and L. Lang, "Dictionary learning for VQ feature extraction in ECG beats classification," *Expert Syst. Appl.*, vol. 53, pp. 129–137, Jul. 2016.

[72] U. R. Acharya, S. L. Oh, Y. Hagiwara, J. H. Tan, and M. Adam, A. Gertych, and. S. Tan, "A deep convolutional neural network model to classify heartbeats," *Comput. Biol. Med.*, vol. 89, pp. 389–396, Oct. 2017.

[73] G. Garcia, G. Moreira, D. Menotti, and E. Luz, "Inter-patient ECG heartbeat classification with temporal VCG optimized by PSO," *Sci. Rep.*, vol. 7, no. 1, p. 10543, Sep. 2017.

[74] S. Chen, W. Hua, Z. Li, J. Li, and X. Gao, "Heartbeat classification using projected and dynamic features of ECG signal," *Biomed. Signal Process. Control*, vol. 31, pp. 165–173, Jan. 2017.

[75] Z. Zhang, J. Dong, X. Luo, K.-S. Choi, and X. Wu, "Heartbeat classification using disease-specific feature selection," *Comput. Biol. Med.*, vol. 46, pp. 79–89, Mar. 2014.

[76] S. A. Deevi, C. P. Kaniraja, V. D. Mani, D. Mishra, S. Ummar, and C. Satheesh, "HeartNetEC: A deep representation learning approach for ECG beat classification," *Biomed. Eng. Lett.*, vol. 11, no. 1, pp. 69–84, Feb. 2021.

[77] T. Wang, C. Lu, Y. Sun, M. Yang, C. Liu, and C. Ou, "Automatic ECG classification using continuous wavelet transform and convolutional neural network," *Entropy*, vol. 23, no. 1, p. 119, Jan. 2021.

[78] E. H. Houssein, I. E. Ibrahim, N. Neggaz, M. Hassaballah, and Y. M. Wazery, "An efficient ECG arrhythmia classification method based on Manta ray foraging optimization," *Expert Syst. Appl.*, vol. 181, Nov. 2021, Art. no. 115131.

[79] E. H. Houssein, D. S. AbdElminaam, I. E. Ibrahim, M. Hassaballah, and Y. M. Wazery, "A hybrid heartbeats classification approach based on marine predators algorithm and convolution neural networks," *IEEE Access*, vol. 9, pp. 86194–86206, 2021.

[80] A. Nasim, A. Sbrollini, M. Morettini, and L. Burattini, "Extended segmented beat modulation method for cardiac beat classification and electrocardiogram denoising," *Electronics*, vol. 9, no. 7, p. 1178, Jul. 2020.

AMNAH NASIM (Member, IEEE) received the bachelor's degree in computational science and engineering and the master's degree in electronics engineering from the National University of Sciences and Technology, Islamabad, Pakistan, and the Ph.D. degree in information engineering from Universita Politecnica delle Marche, Ancona, Italy, in 2021. She is currently a Postdoctoral Researcher at KOREATECH, Cheonan-si, Republic of Korea. Her research interests include affective computing, physiological data monitoring and assessment, and automatic processing of digital cardiovascular signals (electrocardiograms) acquired using wearable sensors. She is a member of GNB.

DAVID C. NCHEKWUBE (Graduate Student Member, IEEE) received the bachelor's degree in electronic engineering from the University of Nigeria, Nsukka, Nigeria, the master's degree in mechatronic engineering from the Politecnico di Torino, Turin, Italy, and the master's degree in biomedical engineering from Universita' Politecnica delle Marche (UNIVPM), Ancona, Italy. He is currently a Research Fellow of the Department of Information Engineering, UNIVPM. His research interests include assistive robotics, human–computer interaction, signal processing, and predictive maintenance.

FARZEEN MUNIR (Graduate Student Member, IEEE) received the bachelor's and master's degrees in electrical engineering from the Pakistan Institute of Engineering and Applied Sciences, Islamabad, Pakistan. She is currently pursuing the Ph.D. degree with the School of Electrical Engineering and Computer Science, Gwangju Institute of Science and Technology, Gwangju, Republic of Korea. Her current research interests include machine learning, deep neural networks, autonomous driving, and computer vision.

YOON SANG KIM (Member, IEEE) received the B.S., M.S., and Ph.D. degrees in electrical engineering from Sungkyunkwan University, Seoul, South Korea, in 1993, 1995, and 1999, respectively. He was a member of the Postdoctoral Research Staff of the Korea Institute of Science and Technology (KIST), Seoul. He was a Faculty Research Associate with the Department of Electrical Engineering, University of Washington, Seattle, USA. He was a member of the Senior Research Staff, Samsung Advanced Institute of Technology (SAIT), Suwon, South Korea. Since March 2005, he has been a Professor at the School of Computer and Science Engineering, Korea University of Technology Education (KOREATECH), Cheonan-si, South Korea. Also, he has been an Affiliated Assistant Professor with the Department of Electrical Engineering, University of Washington, since September 2014. He has directed the Biocomputing Laboratory and the Institute for Bioengineering Application Technology (IBAT). His current research interests include virtual simulation, power-it technology, robotics, and bio-informatics. He is a member of IEICE, ICASE, KIPS, and KIEE. He was awarded the Korea Science and Engineering Foundation (KOSEF) Overseas Postdoctoral Fellow, in 2000.